

Heavy quarkonia survival in potential model

Á. Mócsy^{1,a}, P. Petreczky²

¹ Frankfurt Institute for Advanced Studies, J.W. Goethe-Universität, Postfach 11 19 32, 60054 Frankfurt am Main, Germany

² Nuclear Theory Group, Department of Physics, Brookhaven National Laboratory, Upton, New York 11973-500, USA

Received: 29 November 2004 /

Published online: 16 March 2005 – © Springer-Verlag / Società Italiana di Fisica 2005

Abstract. We investigate the quarkonia correlators in QCD with no light quarks within a potential model with different screened potentials. Our results for the temperature dependence of the charmonium and bottomonium correlators are qualitatively consistent with existing and preliminary lattice results. We identify however, a much richer structure in the correlators than the one seen on the lattice.

PACS. 11.15.Ha, 11.10.Wx, 12.38.Mh, 25.75.Nq

1 Introduction

Matsui and Satz conjectured that color screening prevents the binding of heavy quarks above the deconfinement transition [1]. This idea inspired the intense investigation of heavy quark bound states in hot strongly interacting medium, as this can test deconfinement. Refinement of this idea led to the identification of a hierarchy in the dissolution pattern, meaning that higher excited states disappear earlier [2, 3].

Recently available numerical analysis of quarkonia correlators and spectral functions carried out on the lattice for quenched QCD [4–6] provided unexpected results: The ground state charmonia, 1S J/ψ and η_c , survive at least up to $1.5T_c$. Not only that these states do not melt at, or close to T_c , as it was expected, but lattice calculations also found very little change in their properties when crossing the transition temperature. In particular, the masses of these states show almost no thermal shift. Furthermore, lattice results indicate [6] that properties of the excited 1P states, χ_c^0 and χ_c^1 , are seriously modified above the transition temperature, and that these states are dissolved already at $1.1T_c$. Preliminary results from the lattice approach for the temperature dependence of the bottomonia correlators are now also available [7] and predict the melting of these states at much higher temperatures than the charmonia states.

The above features are in contrast with existing potential model studies, which predicted that the J/ψ would disappear at around $1.1T_c$ (see for example [3]). There have been some recent attempts to understand these results. In [8] the J/ψ was considered as a strongly coupled color-Coulomb bound state and found to survive until $2.7T_c$. In [9] for the J/ψ a spontaneous dissociation temperature of $2T_c$ has been found using a potential fitted

for lattice results. In these studies however, only the question of existence or non-existence of quarkonium binding was addressed. No comparison of the quarkonium properties was made with the available lattice data, although it is expected that these are strongly modified close to the corresponding melting temperatures.

Since the calculation on the lattice of meson spectral functions at finite temperature is difficult even in quenched QCD, we study the quarkonium correlators in QCD with one heavy quark (either c - or b -quark) in terms of a potential model. This allows us to make a direct connection between lattice calculations of quarkonium at finite temperature and potential models.

2 The model

We investigate the quarkonium correlators in Euclidean time at finite temperature, as these are directly calculable in lattice QCD. The correlation function for a particular mesonic channel H is defined as

$$G_H(\tau, T) = \langle j_H(\tau) j_H^\dagger(0) \rangle. \quad (1)$$

Here $j_H = \bar{q}\Gamma_H q$, and $\Gamma_H = 1, \gamma_\mu, \gamma_5, \gamma_\mu\gamma_5$ corresponds to the scalar, vector, pseudo-scalar and axial vector channels. Using its relationship to the retarded correlator, the following spectral representation for $G_H(\tau, T)$ can be derived:

$$G(\tau, T) = \int_0^\infty d\omega \sigma(\omega, T) \frac{\cosh[\omega(\tau - \frac{1}{2T})]}{\sinh[\frac{\omega}{2T}]}. \quad (2)$$

Here we need to specify the spectral function at finite temperature. We do this by following the form proposed in [10] for the zero temperature spectral function,

$$\sigma(\omega) = \sum_i 2M_i F_i^2 \delta(\omega^2 - M_i^2) + m_0 \omega^2 \theta(\omega - s_0). \quad (3)$$

^a e-mail: mocsy@th.physics.uni-frankfurt.de

Table 1. Parameters at $T = 0$

α	σ	m_c	m_b	s_{0c}	s_{0b}
0.471	0.192 GeV ²	1.32 GeV	4.746 GeV	4.5 GeV	11 GeV

The first term contains the pole contributions from resonances, while the second term is the perturbative continuum above some threshold. For QCD with light dynamical quarks it is natural to identify the continuum threshold s_0 with the open charm or beauty threshold. For the case of one heavy quark only, which is considered here, the value of s_0 is somewhat arbitrary. We choose this threshold as the energy above which no individual resonance is observed experimentally. These are shown in Table 1. Our finite temperature model spectral function has the form given in (3), with temperature-dependent decay constant $F_i(T)$, quarkonium mass $M_i(T)$, and threshold $s_0(T)$. For the parameter m_0 we take the value $3/(8\pi^2)$ calculated in leading order perturbation theory [11]. The threshold above which quarks propagate freely is given by twice the effective quark mass, i.e. the temperature-dependent pole mass $s_0(T) = 2m_p(T)$. We consider only the case of zero spatial momentum, and therefore do not have to take into account contributions from Landau damping to the spectral function.

The remaining parameters of the spectral function can be calculated using a potential model. The bound state mass is given by $M_i = 2m_{c,b} + E_i$, where E_i is the binding energy, and $m_{c,b}$ are the constituent charm and bottom quark masses given in Table 1. At leading order in the coupling and inverse mass the decay constant can be related to the wave function at the origin for the vector and pseudoscalar channel, and to its derivative for scalar and axial-vector channels [12]. We obtain the binding energies and the wave functions by solving the Schrödinger equation. We solve this with a temperature-dependent screened Cornell potential, first considered in [2]:

$$V(r, T) = -\frac{\alpha}{r} e^{-\mu(T)r} + \frac{\sigma}{\mu(T)} \left(1 - e^{-\mu(T)r}\right). \quad (4)$$

We parameterize the temperature dependence of the screening mass as $\mu = (0.24 + 0.31 \cdot (T/T_c - 1))$ GeV with $T_c = 0.270$ GeV the critical temperature. Here α is the coupling and σ is the string tension. Their values, as well as the quark masses were obtained in [13] by fitting the zero temperature quarkonium spectrum, and are given in Table 1.

In our analysis we also used a screened potential with a quite different functional form. This was obtained by fitting the quenched lattice QCD data on the internal energy for $T > 1.18T_c$ [14]. We have not considered the internal energy closer to T_c as it is not clear if it can be identified with the potential.

The potential (4) is shown in Fig. 1 for different temperatures above deconfinement. A common feature of all screened potentials is that they reach a finite temperature-dependent asymptotic value, $V_\infty(T)$. This contributes an extra thermal energy to the quark-antiquark pair in the plasma [15]. This thermal internal energy thus leads to an

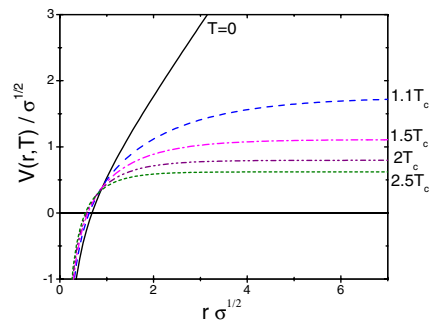


Fig. 1. Cornell potential at $T = 0$ and screened Cornell potential for different $T > T_c$. Here $\sigma = 0.192$ GeV is the zero temperature string tension

effective quark mass given by $m_p(T) = m_{c,b} + V_\infty(T)/2$. Since $V_\infty(T)$ is decreasing with temperature, also $s_0(T) = 2m_p(T)$ will decrease accordingly, the effect of which becomes manifest in the temperature dependence of the correlators, as we discuss in the following section. Such a decrease in the pole mass was observed in lattice calculations [16] when calculating quark and gluon propagators in Coulomb gauge. While we assume that above the threshold quarks and antiquarks propagate with the temperature-dependent effective mass defined above, quarks inside a singlet bound state will not feel the effect of the medium, and thus will have the vacuum mass. Therefore, in the Schrödinger equation we use the zero temperature masses of c - and b -quarks. Above deconfinement the quarkonium can also dissociate via its interaction with gluons [17]. This effect leads to a finite thermal width, which we will neglect in the following analysis.

3 Results

Here we concentrate on results obtained in the scalar and pseudoscalar channels. Details of the analysis, together with the study of the vector channel, where transport effects are also considered, will be presented elsewhere [18].

First, let us discuss the properties of the quarkonia in the deconfined medium. In Figs. 2 and 3 we present the temperature dependence of the masses and the amplitudes $F(T)$ (i.e. the wave function or its derivative at the origin)

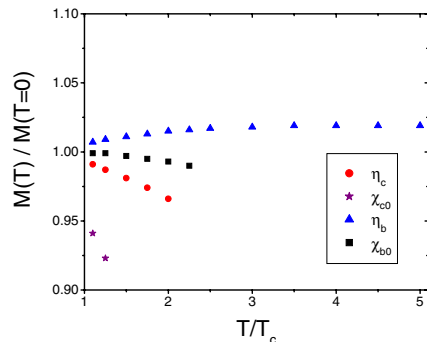


Fig. 2. Temperature dependence of quarkonia masses normalized to their corresponding zero temperature masses

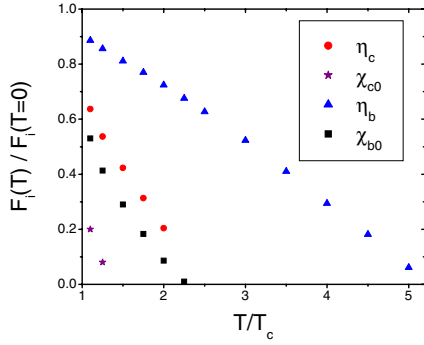


Fig. 3. Temperature dependence of quarkonia amplitudes normalized to their corresponding zero temperature amplitudes

of the different quarkonia states. One can see that while the masses do not change substantially with temperature, there is quite a strong drop in the corresponding amplitudes. While the small shift in the quarkonia masses above the deconfinement temperature is consistent with lattice data, the decrease in the amplitudes is neither confirmed, nor ruled out by existing lattice data.

In order to make a direct comparison with lattice results we normalize the correlation function to the so-called reconstructed correlators [6]:

$$G_{\text{recon}}(\tau, T) = \int_0^\infty d\omega \sigma(\omega, T=0) K(\tau, \omega, T). \quad (5)$$

Studying the ratio G/G_{recon} can indicate the modifications of the spectral function above T_c . Deviations of this ratio from one is an indication of medium effects.

The results for the scalar χ_c^0 and pseudoscalar η_c charmonia correlators are presented in Fig. 4. There is a very large increase of the scalar correlator (upper panel) which is in qualitative agreement with lattice data [6]. The scalar correlator above deconfinement is enhanced compared to the zero temperature correlator despite the fact that the contribution from the χ_c^0 state becomes negligible. This enhancement is due to the thermal shift of the continuum threshold. For the pseudo-scalar correlator (lower panel) we also find a moderate increase. This increase of the correlator is again attributed to the decrease of the threshold with temperature. This extra feature, i.e. the significant contribution to the correlator from the continuum due to threshold reduction, is not detected on the lattice for the pseudoscalar channel.

A qualitatively similar behavior was obtained for the bottomonia states, χ_b^0 and η_b , as illustrated in Fig. 5. The behavior of the scalar bottomonium channel is very similar to that of the scalar charmonium, even though contrary to the χ_c^0 state the χ_b^0 survives until much higher temperatures. This is due to the fact that the shifted continuum gives the dominant contribution to the scalar correlator. In the pseudoscalar channel we see a drop in the correlator at large enough distance compared to the zero temperature correlator which is due to the reduction of the amplitude. This is presumably due to the fact that 1S bottomonia are more deeply bound; thus there is a clearer separation between the pole and continuum contributions to the correlator.

In the analysis presented so far we have considered only the lowest meson state in a given channel. This is because we wanted to make contact with existing lattice data in which the excited states in any given channel were

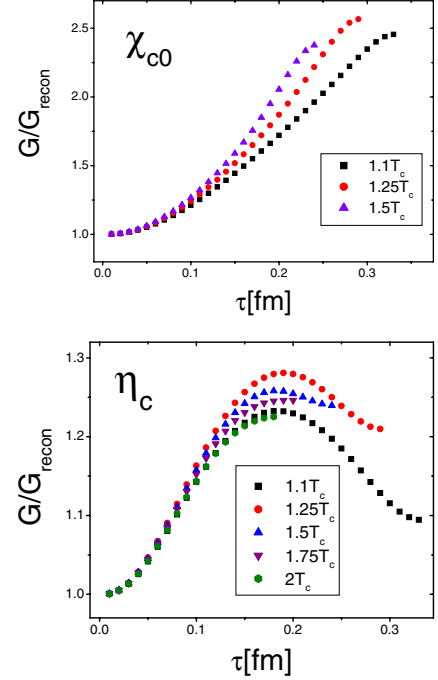


Fig. 4. Ratio of charmonia correlators to reconstructed correlators for scalar (upper panel) and pseudoscalar (lower panel) channels

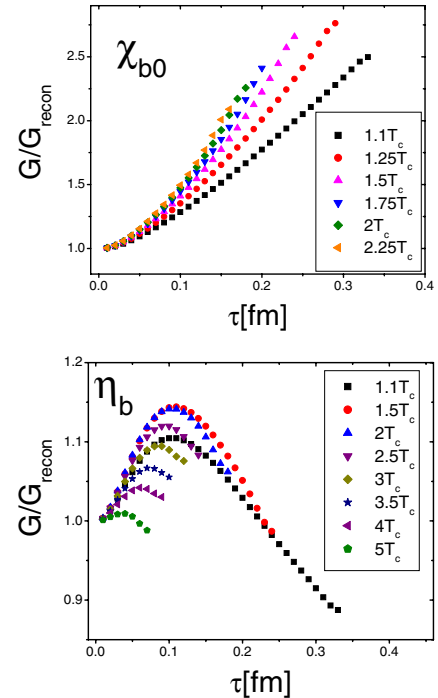


Fig. 5. Ratio of bottomonia correlators to reconstructed correlators for scalar (upper panel) and pseudoscalar (lower panel) channels

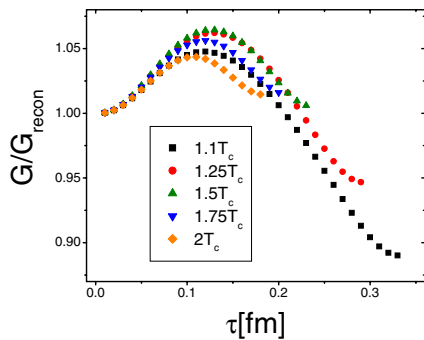


Fig. 6. Ratio of the pseudoscalar charmonia correlator to the reconstructed correlator that includes 1S and 2S states

not yet observed. To study possible effects due to higher states in a given channel we have included also the 2S state in the pseudoscalar channel in the spectral function (3). Since the 2S state is melted at T_c , we expect a drop in G/G_{recon} compared to the previous case, where only the 1S state is included. Figure 6 shows the temperature dependence of the charmonium pseudoscalar correlator obtained when both the 1S and the 2S states are accounted for. As expected, in this case we identify a 25% reduction in the correlator, attributed to the melting of the 2S state. This has not been seen on the lattice, since data involving the 2S state are still unavailable.

To test the robustness of our results we reconsidered the analysis with a different parameterization of the screening mass. For temperatures $T > 1.18T_c$ we also used the potential fitted to the internal energy calculated on the lattice. Our results proved not to be sensitive to the detailed form of the potential, suggesting that they are based on very general physical arguments [18].

In conclusion: We have analyzed mesonic correlators using model spectral functions based on the potential picture with screening. We have found qualitative agreement with lattice data. On the other hand the temperature dependence of the correlators shows a much richer structure than the one seen on the lattice.

Acknowledgements. We thank A. Dumitru, R. Pisarski, H. Satz, and I. Shovkovy for inspiring discussions. A.M. thanks the Theoretical Physics Institute at J.W. Goethe University in Frankfurt, and RIKEN at Brookhaven National Laboratory for the hospitality extended to her during the course of this work. This work was partly supported by U.S. Department of Energy under contract DE-AC02-98CH10886. A.M. is a Humboldt Fellow. P.P. is a Goldhaber and RIKEN-BNL Fellow.

References

1. T. Matsui, H. Satz, Phys. Lett. B **178**, 416 (1986)
2. F. Karsch, M.T. Mehr, H. Satz, Z. Phys. C **37**, 617 (1988)
3. S. Digal, P. Petreczky, H. Satz, Phys. Rev. D **64**, 094015 (2001) [hep-ph/0106017]
4. T. Umeda, K. Nomura, H. Matsufuru, [hep-lat/0211003]
5. M. Asakawa, T. Hatsuda, Phys. Rev. Lett. **92**, 012001 (2004) [hep-lat/0308034]
6. S. Datta, F. Karsch, P. Petreczky, I. Wetzorke, Phys. Rev. D **69**, 094507 (2004) [hep-lat/0312037]
7. K. Petrov, [hep-lat/0503002]
8. E.V. Shuryak, I. Zahed, Phys. Rev. C **70**, 021901 (2004) [hep-ph/0307267]; [hep-ph/0403127]
9. C.Y. Wong, [hep-ph/0408020]
10. E.V. Shuryak, Rev. Mod. Phys. **65**, 1 (1993)
11. L.J. Reinders, H. Rubinstein, S. Yazaki, Phys. Rep. **127**, 1 (1985)
12. G.T. Bodwin, E. Braaten, G.P. Lepage, Phys. Rev. D **51**, 1125 (1995) [Erratum D **55**, 5853 (1997)] [hep-ph/9407339]
13. S. Jacobs, M.G. Olsson, C.I. Suchyta, Phys. Rev. D **33**, 3338 (1986) [Erratum D **34**, 3536 (1986)]
14. O. Kaczmarek, F. Karsch, P. Petreczky, F. Zantow, Nucl. Phys. Proc. Suppl. **129**, 560 (2004) [hep-lat/0309121]
15. S. Digal, P. Petreczky, H. Satz, Phys. Lett. B **514**, 57 (2001) [hep-ph/0105234]
16. P. Petreczky, F. Karsch, E. Laermann, S. Stickan, I. Wetzorke, Nucl. Phys. Proc. Suppl. **106**, 513 (2002) [hep-lat/0110111]
17. D. Kharzeev, H. Satz, Phys. Lett. B **334**, 155 (1994) [hep-ph/9405414]
18. Á. Mócsy, P. Petreczky, in preparation